Journal of Applied Polymer Science

Effect of Extruder Elements on Fiber Dimensions and Mechanical Properties of Bast Natural Fiber Polypropylene Composites

Ahmed Mohammed Moneeb El-Sabbagh,[1,2] Leif Steuernagel,[1] Dieter Meiners,[1] Gerhard Ziegmann[1]

[1]Institute for Polymer Materials and Plastics Engineering, Agricolastrasse 6, 38678 Clausthal-Zellerfeld, Germany

[2]Design and Production Engineering Department, Faculty of Engineering, Ain Shams University, Egypt

Correspondence to: A. M. M. El-Sabbagh (E-mail: ahmed.sabbagh@tu-clausthal.de)

ABSTRACT: Illusions and facts about aspect ratio and the corresponding mechanical properties of the polypropylene flax are studied in this work. Selection of extruder elements controls significantly the fiber final dimensions. Hence, the load transfer efficiency can be improved. Different extruder layouts are tried. First and second trials investigate the mixing degree effect using kneading elements with eight and four kneading elements, respectively. The third and fourth trials keep four kneading blocks but differentiate in using multiprocessing element MPE and toothed elements, respectively. All the four configurations are tested at different shearing rates namely 100, 200, and 300 rpm and different fiber loadings 10, 20, and 30 wt %. Polypropylene (PP) with high flowing properties and slivers flax natural fibers are used. The output extruded strands are mechanically tested. The third and fourth configurations showed superiority to the normal kneading profiles regarding the mechanical properties. Samples of composites are withdrawn after each processing extruder element to study the effect of this element on the fiber dimension. Measurement of extracted fibers is carried out by two methods namely dynamic image analysis machine and secondly normal microscopic investigation. Weibull distributions are defined for fiber geometry distributions for the different locations on the extruder configuration. Also, the effect of the shear rate and the extruder configuration on the final dimensions of the fibers extracted from the composite. The results show the correlation between extruder configuration and fiber aspect ratio and hence the composite overall strength. However, further processing like injection molding erases the pre-extrusion effect. © 2014 Wiley Periodicals, Inc. J. Appl. Polym. Sci. **2014**, *131*, 40435.

KEYWORDS: extrusion; fibers; mechanical properties; biomaterials

Received 7 September 2013; accepted 13 January 2014

DOI: 10.1002/app.40435

INTRODUCTION

Implementation of the natural fibers as reinforcement for polymers in different industrial applications receives a remarkable attention.[1,2] The main advantages of natural fibers are their low density, availability, suitability to be processed by the normal technology (i.e. extrusion, injection molding, and pultrusion) and their low abrasion during processing in comparison with glass fiber.[3] Glass and carbon fibers are herewith in part replaced with the environment friendly natural fibers. However, some problems arise with the use of natural fibers such as the increased water absorption and lack of adhesion between the fiber and matrix.[4] Compounding of thermoplastic polymers with natural fibers takes place most likely in extruders to achieve mass production. The mechanical properties of the extruded composite are improved by avoiding the following factors. First, if the fiber thermal degradation is due to overheating or severe shearing, consequently, the fibers' mechanical properties like E-modulus and strength will be reduced. Second, the bad fiber-matrix adhesion, which can negatively affect the effectiveness of polymer fiber load transfer.[5] Third, the inhomogeneous distribution of fibers within the host thermoplastic matrix, which will result in local week areas. Finally, the fiber length to diameter ratio; which is the fiber aspect ratio. Low aspect ratio (normally <20) is thoroughly studied using the fibers reinforcing concept.[6–8] Modeling of the mechanical properties of the fiber filled polymeric composites originates mainly from the rule of mixture concept. This simple rule is exposed to many modifications[5,8,9] regarding the fiber length, orientation and coverage efficiency with the coupling agent. fiber and orientation efficiency factors are introduced in Kelly-Tysson formula, eq. (1) for both E-modulus and strength.[7] They are found to give more matching with the experimental results.[8,9] Other modifications are suggested and implemented by El-Sabbagh et al.[9]

$$\sigma_c = \sigma_m(1-v_f) + \eta_{oE}\eta_{lE}\sigma_f v_f \quad (1)$$

where subscripts '*c*', '*m*', and '*f*' stand for composite, matrix and fiber respectively, v_f is the fiber volume fraction, 'σ' is strength, '*o*' and '*l*' stand for orientation and fiber.

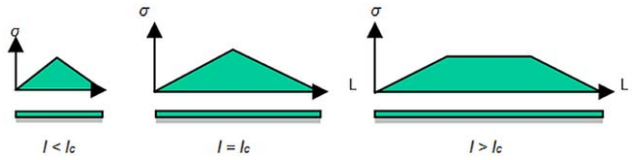

Figure 1. Effect of fiber length on fiber capacity for load transfer. [Color figure can be viewed in the online issue, which is available at wileyonlinelibrary.com.]

Efficiency terms for the fiber length are defined in eq. (2). Figure 1 shows the effect of fiber length with respect to the fiber critical length (fiber length or aspect ratio at certain diameter corresponding to the maximum load transfer)

$$\eta_{l\sigma}=\begin{cases}1-\dfrac{l_c}{2l}\cdots l\geq l_c\\ \dfrac{l}{2l_c}\cdots l<l_c\end{cases} \quad (2)$$

l_c is the critical fiber length at which the fiber loading efficiency is maximized. It is defined in eq. (3)

$$l_c=\frac{\sigma_f d}{2\tau} \quad (3)$$

σ_f is the fiber strength, d is the fiber diameter and σ is the interfacial shear strength.

Most of the researchers used the mean values of the fiber lengths.[8–11] Only Andersons et al.[12] who has used Weibull distribution in order to describe the fiber length population and hence to define the fiber portions below and above the critical fiber length. Andersons et al. investigated extruded flax roving-polypropylene composites at 180–200°C at ZSK 25 WLE twin screw extruder. Some conditions of the extruder are missing namely; speed and extruder elements. The effect of different extruder designs and shear rates was not studied by Andersons et al.[12] However, some trials to explore the effect of the extruding element on the aspect ratio were discussed by El-Sabbagh[13] and Beaugrand and Berzin.[14]

Beaugrand and Berzin[14] carried out experiments on low melting polymer PCL with chopped Hemp fibers using severe and light kneading configurations at different speeds, temperature and feeding rates. The effect of the fiber failure method by fragmentation in the cell wall or the decohesion in the interfiber cement was correlated with the fiber aspect ratio. Beaugrand and Berzin[14] expected firstly that there will be a linear trend relation between fiber aspect ratio and the mechanical property. Thus, the severe kneading screw configuration should result, according to the expectation, in low aspect ratio however the breaking stress was surprisingly higher than that of the light kneading configuration. Beaugrand and Berzin[14] justified his finding that L/D ratio does not give full description of stress transfer. He expected that lower aspect ratio with more defibrillation (as a result of severe kneading) creates more load-bearing interfaces and hence higher breaking stress is attained. However, it should be recalled that PCL processing temperature is less than the temperature profile in PP natural fiber composites presented in this study. Therefore, the fiber fracture modes will be increased; especially, the decohesion where the energy needed to dissolve the cement wall bonding will be definitely reduced.

The current work will address the possible control of fiber geometry distribution (diameter, length, and hence the aspect ratio) using different extruder layout designs and different shear rates (extruder speeds) at different fiber loadings and extrusion ratios.

EXPERIMENTAL

Material Preparation

Flax fibers were supplied by Sachsenleinen-Germany in sliver. The lengths of fibers vary from 100 to 500 mm and diameter of 68 μm in average with overall specific gravity of 1.4. Homopolymer polypropylene PP supplied by DOW company (Melting flow index = 52). Carboxylated polypropylene (maleic anhydride) MAPP as a coupling agent is supplied by Kometra with a product name of Scona TPPP 8112 FA (MFI = 80 g/10 min at 190°C/2.16 kg) suitable for wood and natural fiber composites with polypropylene.

Flax slivers are cut to 10 m length, then alkalinized with a solution of 2% sodium hydroxide overnight. The fibers are then washed with distilled water and neutralized. Drying takes place in two steps: first left in ambient air for 24 h and then left at 80°C for another 24 h.

MAPP is mixed with PP bearing in mind that MAPP : Flax is 1 : 10 wt/wt. Figure 2 illustrates the sequence of compounding where the PP/MAPP previously mixed are fed through input hopper and then the fibers are inserted from the extruder side opening. The temperature pattern is 180–190–190–200–210–220–230–230°C from input to output zones.

Table I illustrates the plan of the investigated parameters namely; speed, fiber content and extruder layout. Screw layout effect is investigated in four arrangements. The common feature between the extruder designs is the use of the conveying elements with descending width pitches (37.5–25 mm pitch) in order to ensure material transport at the beginning then pressure build-up in the metering section at the output die. Second common feature is the presence of reverse element to produce a significant back pressure and to guarantee that the elements in front of the reverse element are fully filled with the melt.

Layouts (A) and (B) have different numbers of kneading elements which are responsible of mixing. Only kneading elements that deal with the input fibers are considered. The kneading elements at the feed zone which deal only with the polymer granulates are not considered. The used kneading block is unified through all the extruder designs which is 25/5/45L (25 mm length with 5 discs left hand rotated at 45° in subsequent order). One layout (A) with eight kneading elements and another with four kneading blocks (B). Screw (C) contains patented multiprocess elements (MPE) which allows soft incorporation of shear sensible fibers into the polymer flow. The openings in the MPE element reduce the high shear forces applied on the fibers. MPE also allows the extrusion of moist wood flour/fibers or bast fibers. The direct processing of fibers without predrying also eliminates any risk of explosion. The

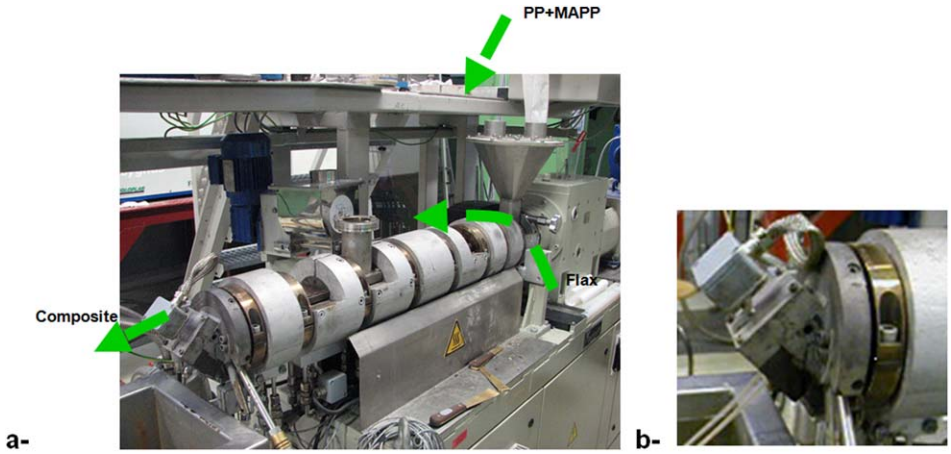

Figure 2. Compounding procedure of PP and natural fiber at Berstorff ZE25Ax40D. (a) Overall photo, (b) extruded two strands. [Color figure can be viewed in the online issue, which is available at wileyonlinelibrary.com.]

section of MPE elements was composed of right and left handed elements to act as a mixing element for the material flowing forward and backward.

Screw (*D*) with teethed blocks cause fibers cutting during entry and reversed flow which in turn helps in better fiber compounding. The different design layouts of the used extruders are shown in Figure 3. Different fiber contents are tested namely 10, 20, and 30 wt%. fiber content is calculated and not adjusted directly by the extruder control panel. That is because the fibers are fed as a sliver to the ingate at one-third of the extruder length directly to the screw housing.

fiber content inside the composite is estimated through the control of the parameters of fiber linear density (W_{NF}), screw speed (n), thermoplastic granulates feed rate ($\dot{W}_{pp}$) and finally a constant (a) which is related to the geometry of the extruder. All of these are connected in eq. (4).

$$w_{NF} = \frac{w_{NF}}{w_{NF}+w_{pp}} = \frac{\dot{w}_{NF}}{\dot{w}_{NF}+\dot{w}_{pp}} = \frac{1}{1+\frac{\dot{w}_{pp}}{\dot{w}_{NF}}} = \frac{1}{1+\frac{\dot{w}_{pp}}{a\frac{\partial w_{NF}}{\partial x}n}} \quad (4)$$

Shear rate (screw speed) effect is also carried out at 100, 200, and 300 rpm. The exit die produces two round cross-sectional composite profile which is 1 : 10 extrusion ratio seen in Figure 3(b).

Mechanical Specimen Preparation Out of Extruded Material

To measure the mechanical properties of the extruded material without further shearing or fiber damage, the extruded strands are laid in a dog bone and then hot pressed at 500 bar and 200°C. Then, the effect of further processing is studied by cutting the extruded strands of composites using a mechanical shredder. Then the attained granulates are then injection molded at a temperature pattern of 185–190–195–200°C, while the conditioning is applied for all specimens at 23°C/50% relative humidity for 88 h according to DIN EN ISO 179-1. Tension tests were made with at least five samples using Zwick 0.2 ton tensile machine according to DIN EN ISO 527-1 at 2 mm/min testing rate.

Table I. Plan of Work

Parameter	Alternatives
Screw layout	A/B/C/D
Screw speed [rpm]	100/200/300
fiber content [wt %]*	10/20/30

Samples for Fiber Geometry Development Along Extruder Length

To observe the fiber geometry development along the extruder processing, the extruder is stopped during the feeding process of the fiber bundle into the extruder. The screw is then withdrawn out of the extruder housing. Then, samples are taken from the fibers sticking to the screw at the positions that are directly after each element within the screw as shown in Figure 4.

Dynamical Image Analysis Method. It is a more precise way to measure the fiber length and diameter. The fibers should be extracted from the composite by decalin solvent. The sample is weighed before and after the test to calculate the fiber content. The extracted fibers from each spot are then air pressurized at 4 bar by the dry dispersing unit (Rodos/L) using the Qicpic machine. The fibers are blown through a light beam and collected finally at the suction. The experiments are done using two types of lenses; namely, M8 (20–6820 μm) and M6 (5–1750 μm) according to ISO 13322-2. Each test is repeated twice because bigger lens is suitable for fiber length and the smaller lens is more accurate for the diameter measurement.

Microscopic Examination. Each sample is squeezed between two heated plates at 180°C enveloped with glossy paper to obtain a thin film. fibers in the thin film can be easily measured using an optical microscope. Fifty measurements are taken at least for the diameter and the corresponding length and hence the aspect ratio is calculated.

Effect of Injection Molding on the Composite Mechanical Properties and Fiber Geometry

The extruded composites are cut using a mechanical shredder and then injection molded at a temperature pattern of 185–190–195–200°C, while the conditioning is applied for all

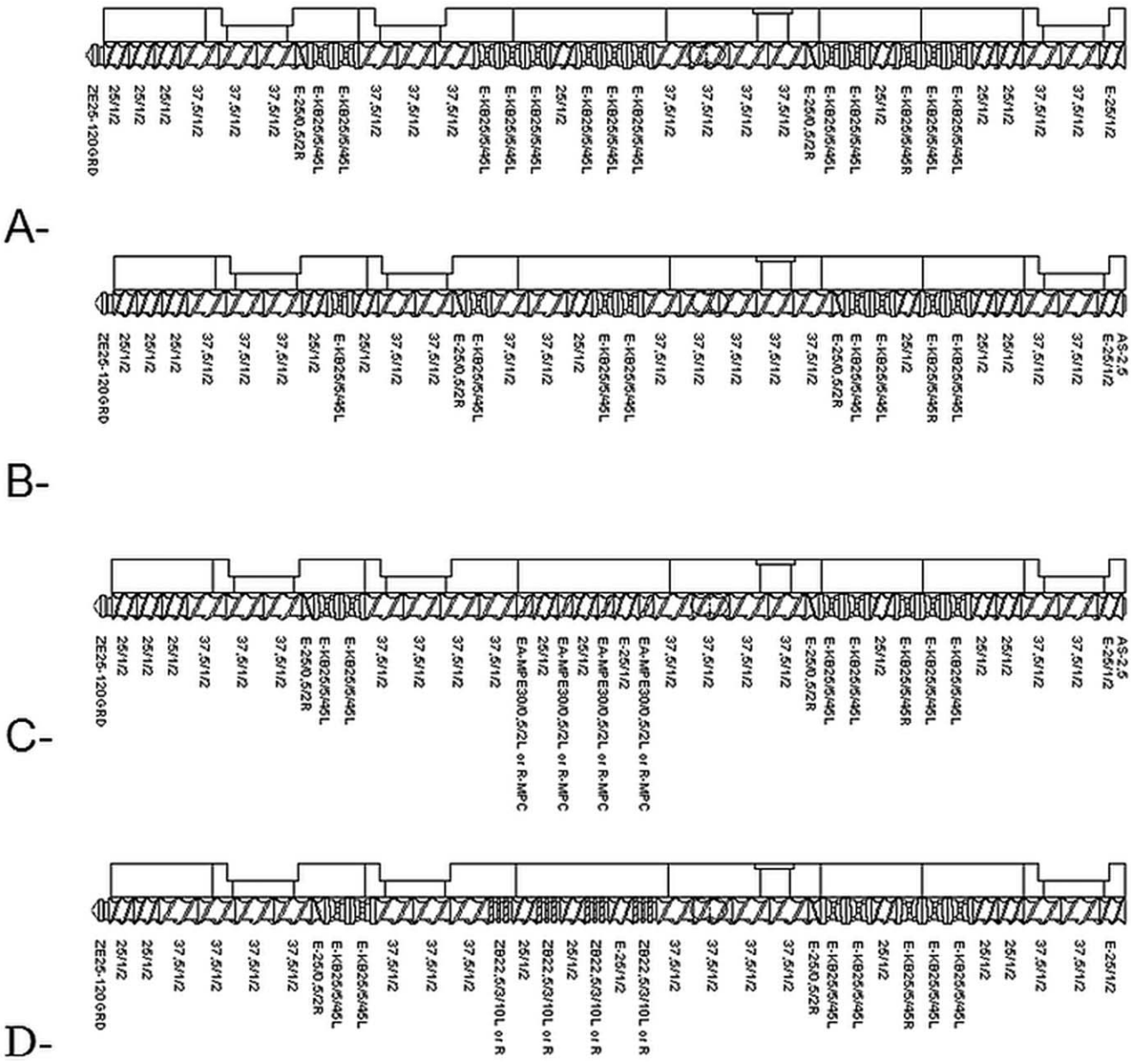

Figure 3. Extruders layouts of A/B/C/D.

specimens at 23°C/50% relative humidity for 88 h according to DIN EN ISO 179-1.

RESULTS AND DISCUSSION

Fiber Content Validation

The fibers in the extruded samples are extracted and hence the actual fiber content is calculated. The actual fiber contents are then compared against the theoretical values to check the validity of eq. (4). Figure 5 shows that the error in the trend lines of fiber content estimation is tolerable (almost 5%), regardless the different fiber contents and different screw layouts.

Mechanical Properties

The mechanical properties are mainly presented to show the effect of extruder configuration on the composite. However,

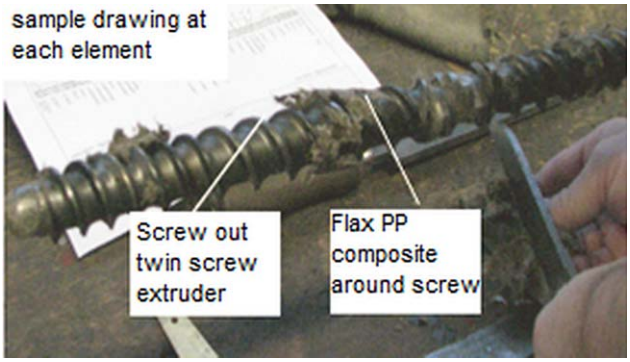

Figure 4. Sample taken at the end from each element after stopping the extruder and drawing the screw. [Color figure can be viewed in the online issue, which is available at wileyonlinelibrary.com.]

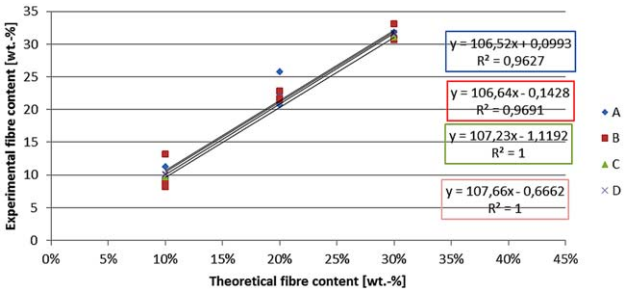

Figure 5. Comparison between the real and the theoretical fiber contents. [Color figure can be viewed in the online issue, which is available at wileyonlinelibrary.com.]

further processing, namely injection molding, is carried out to explore the effect of further shear processing on the composite mechanical properties. Therefore, the results in the next section will be classified to the mechanical properties of the extruded materials and those of the injection molded materials. The following section will try to interpret the attained mechanical properties and the fiber dimensions in terms of the processing parameters and the extruder configurations.

Hot Pressed Samples Out of Extruded Strands. Table II presents the E-modulus, tensile strength, and total elongation measured for the tensile specimens made from hot pressing of extruded strands. Figure 6 shows the tensile testing results with respect to the fiber content for the different speeds and the different extruder configurations. Increase in fiber content leads to an increase in E-modulus as well as for strength as shown in Figure 6(a,b). In case of strength it seems that the behavior follows a parabolic function where the maximum strength takes place at [20–30] wt % depending on the shape of the configuration. The reported strength values are less than that reported in literature.[15] This is because the kneaded composites reach higher levels of fiber distribution and adhesion with the host matrix; especially, under the used high injection pressure, whereas the extruded/pressed samples have more weakness points like fiber agglomerations, lack of adhesion and incomplete mold filling during hot pressing.

E-modulus and tensile strength show roughly that the ranking of the extruder configurations from the lowest to the best is as follows: B-A-D-C. The strain at break is oppositely ranked where the 'C' configuration has the least strain and 'B' has the maximum strain. The reasons of the improved strength and E-modulus in configuration 'C' can be explained by either of the following reasons: Higher fiber aspect ratio because of the soft compounding profile reached by the MPE elements, or due to more available sites on the fiber surface area and hence more free hydroxyl groups that couple with PP in occurrence of MAPP.[16] The share of each reason can be hereafter discussed and justified after measuring the geometry of the extracted fibers. Configuration (D) has the next performance. This is can be explained in terms of the openings within the teeth elements which play a similar role to MPE elements. However, the teethed blocks assert some damage for the fibers by shortening them mechanically and not by decohesion as preferred. This suggests that teethed block of configuration (D) can reach that of configuration (C) only if the design of the teeth openings is justified. Thus may be useful to handle natural fiber slivers which are fed from the extruder side.

The other configurations (A) and (B) have lower mechanical properties in comparison with extruders (C) and (D). This implies that MPE and teethed elements play better rule in strengthening. This may be attributed to better defibrillation or better mixing by more adhesion areas. Both assumptions will be discussed in the fiber measurement section. Regarding extruders (A) and (B) with severe and light kneading, the results in Figure 6(a,b) show that severe kneading leads to higher mechanical properties (in comparison with light kneading configuration). It can be depicted that the severe kneading results in more fibrillation leading to more adhesion area between PP and natural fibers and hence a better load transfer is achieved. Light kneading in configuration (B) is expected to result in larger fiber agglomerations and less adhesion area with the host PP matrix and thus less load capacity. On the other hand, the elongation at break of configuration (B) is found to be the maximum. That is because of the lower fibrillation grade in the light kneading case. Less fibrillation allows significant slide of fiber-to-fiber under stress. Also, local defects due to incomplete polymer impregnation would cause more discontinuities in fiber matrix contact which in turn allows only polymer and not fiber straining. It would be useful in the future to carry out some experiments on the effect of more kneading elements on the fiber length/diameter and the corresponding mechanical properties to see which trend will be followed by these relations namely linear or nonlinear.

Figure 7 presents the results again but with respect to the applied speed. Except configuration (A) at 20 and 30%, there is no significant effect for speed on E-modulus as presented in Figure 7(a). Meanwhile the effect of increasing speed on strength, Figure 7(b), seems significant and negative especially in the speed range [100–200] rpm. Another notice is that the 30% fiber loading is the least affected by the speed change. It is also obvious in Figure 7(a,b); that the behavior of 30% fiber loading seems superior regarding E-modulus and strength in comparison with 10 and 20% for the whole speed spectrum. 10 and 20% have overlapping behavior along the different speeds. This suggests the nonlinearity between fiber content and the measured mechanical property. The results of screw speed effect on E-modulus and strength match partially with what reported by Beaugrand and Berzin[14] where no significance is found for the range of [100–400] rpm.

Figure 7(c) shows the speed effect on the elongation at break. The trend appears from the first glance that it is not consistent. However, a deep insight shows that configurations (A) and (B) at 10 and 20% have an improvement trend in the range of [100–200] rpm. This suggests that there are two contradicting factors. More speed enhances the distribution of fibers homogeneously. But on the other side, the fiber length is shortened and hence the load transfer is weakened.

Injection Molded Samples. Figure 8(a) shows the tensile strength results after the injection molding with respect to the fiber content for the different extruder configurations. This

Table II. Mechanical Properties of the Hot Pressed Samples Out of Extrusion

Extruder	Theoretical fiber content (wt %)	Speed (rpm)	E-modulus (MPa)	Standard deviation (MPa)	Ultimate tensile strength (MPa)	Standard deviation (MPa)	Strain at break (%)	Standard deviation (%)
A	10	100	753.1	138.3	16.04	2.400	3.64	0.79
A	20	100	1327.0	140.3	21.20	2.523	2.31	0.73
A	30	100	964.3	215.1	19.81	4.817	2.13	0.83
A	10	200	786.8	205.0	19.12	3.676	4.90	2.43
A	20	200	655.8	157.1	13.98	1.755	2.96	0.92
A	30	200	1227.0	252.3	18.58	5.139	1.74	0.69
A	10	300	762.4	164.2	16.21	2.793	4.25	0.9
A	20	300	963.0	237.5	19.09	4.348	3.36	0.75
A	30	300	1025.0	184.4	16.33	5.103	1.54	0.82
B	10	100	782.2	94.52	16.27	3.039	3.78	1.77
B	20	100	495.7	84.26	15.22	4.342	3.56	0.96
B	30	100	1003.0	256.1	19.62	5.693	3.01	0.90
B	10	200	700.0	100.0	11.19	2.247	4.31	1.33
B	20	200	489.9	130.6	11.69	1.985	4.48	1.33
B	30	200	960.1	226.0	16.94	3.178	2.39	0.83
B	10	300	651.4	163.8	15.56	4.924	4.44	1.18
B	20	300	577.9	168.1	12.70	3.867	3.17	1.12
B	30	300	824.4	230.1	15.96	4.222	1.87	0.48
C	10	100	1354.0	282.2	28.41	5.316	3.58	1.01
C	20	100	1435.0	356.2	32.91	7.539	2.27	1.30
C	30	100	1515.0	127.4	26.32	4.040	2.35	0.84
C	10	200	1140.0	364.9	22.09	2.997	2.70	2.01
C	20	200	1435.0	356.2	26.33	7.539	2.27	1.30
C	30	200	1603.0	398.2	24.64	6.715	1.94	0.59
C	10	300	1515.0	153.4	23.45	5.137	3.62	0.42
C	20	300	1435.0	87.7	25.6	2.698	2.37	0.80
C	30	300	1603.0	398.2	24.64	6.715	1.94	0.59
D	10	100	1039.0	56.16	26.17	1.192	4.00	0.64
D	20	100	989.2	230.7	17.77	8.395	3.40	0.68
D	30	100	1421.0	246.1	21.47	1.084	2.16	0.79
D	10	200	1037.0	150.4	21.58	3.098	3.60	0.82
D	20	200	989.2	230.7	17.77	8.395	3.40	0.68
D	30	200	1264.0	247.3	20.89	3.887	1.95	0.55
D	10	300	1235.0	221.3	24.05	4.522	2.97	1.25
D	20	300	1101.0	287.4	16.86	8.061	2.76	0.60
D	30	300	1150.0	276.8	20.38	5.019	2.29	0.55

time, the effect of fiber content is completely significant in comparison to the behavior shown in Figure 6. However, the rate of improvement seems to change from one configuration to another. Configurations (A) and (B) show linear improvement with steep increasing gradient with respect to fiber content. This can be attributed to their weak strength nature in the pressed/extruded case. Therefore, just further hot shearing during injection molding process has induced this improvement. On the other side, configurations (C) and (D) did not show such improvement with low shearing rate at 100 rpm. This behavior suggests that the fiber geometry and distribution was already good in the first processing phase (extrusion) so that no significant improvement is observed after injection molding. This infers that fiber aspects did not alter significantly after injection molding at shear rate of 100 rpm. It is also obvious that at 30% fiber content; the effect of speed is totally insignificant for configurations (A) and (B) where all speeds' curves coincide together as enclosed in the shown circles. This may be attributed to the reached level of severe fiber damage due to excessive friction in 30% fiber content by configurations (A)

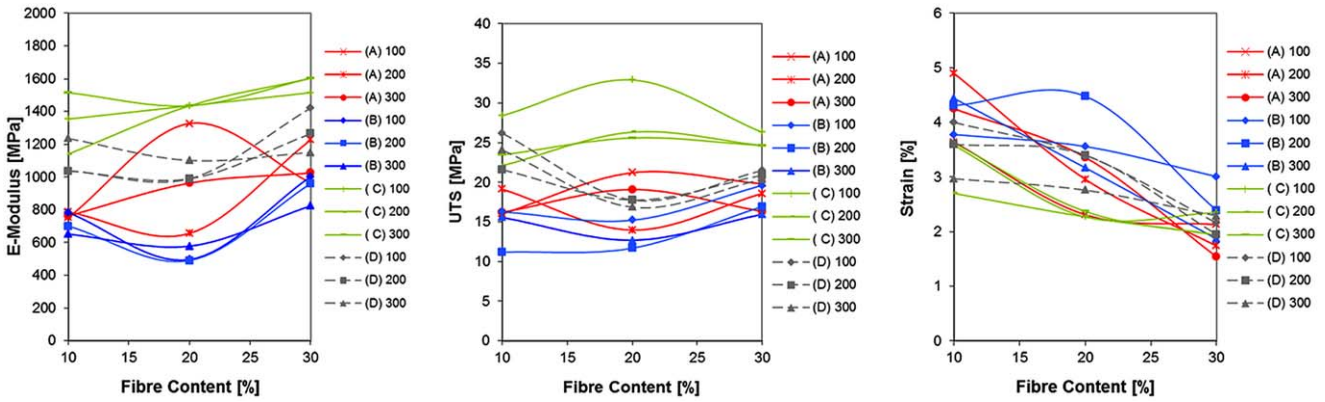

Figure 6. Tensile testing results with respect to fiber content. (a) E-modulus, (b) tensile strength, and (c) strain at break. [Color figure can be viewed in the online issue, which is available at wileyonlinelibrary.com.]

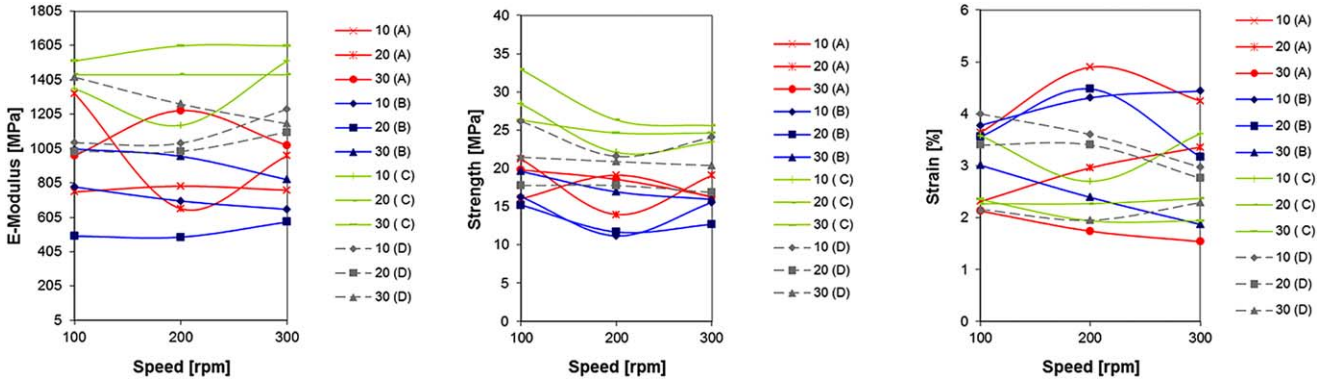

Figure 7. Tensile testing results with respect to speed. (a) E-modulus, (b) tensile strength, and (c) strain at break. [Color figure can be viewed in the online issue, which is available at wileyonlinelibrary.com.]

and (B). Although the configurations (C) and (D) show that there is a difference between strengths of the composites reinforced with 30% fiber at the different applied speeds.

Figure 8(b) shows the improvement ratio of the tensile strength by dividing the injection molded strength to the strength of the pressed strands. The improvement is maximized in case of the configurations (A) and (B) and minimum by configuration (C). Configuration (D) improvement level lies between those of configurations (C) and (A). The improvement is in all cases positive (>100%) which implies the enhancement of the adhesion between fiber and polypropylene and the distribution pattern of the natural fibers in the polypropylene matrix. But from another way, the minimum improvement of configuration (C) suggests that we can reach the required mechanical properties

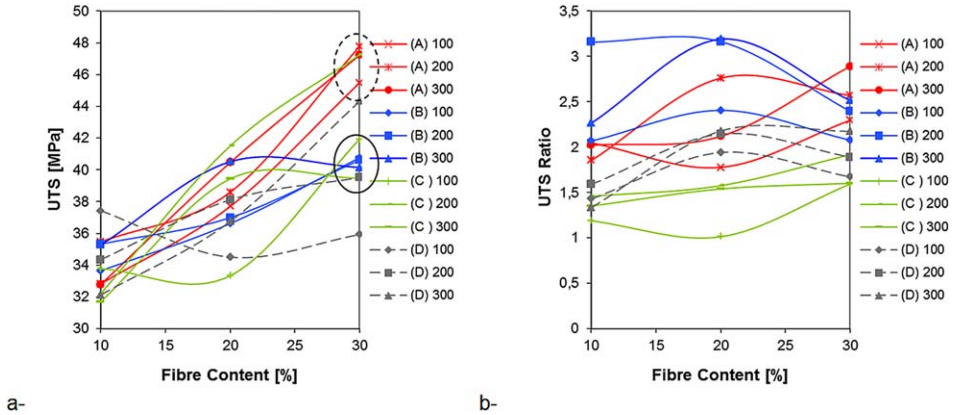

a- b-

Figure 8. Tensile testing results after injection molding. (a) E-modulus, (b) tensile strength, and (c) strain at break. [Color figure can be viewed in the online issue, which is available at wileyonlinelibrary.com.]

Table III. Measured Fiber Diameter/Length from the Accumulated Frequency Curves for All Extruders and the Final Aspect Ratio

Extruder	Fiber (wt.%)	rpm	Number of fibers	×(10%)	×(50%)	×(90%)	×90/×10 LEFI	AR
A	10	100	6000	5.36/36.00	9.90/200.07	18.64/1300.00	3.47/36.11	20.22
A	10	200	6570	5.76/37.11	9.60/195.73	19.20/1397.15	3.33/37.65	20.39
A	10	300	8630	5.33/22.33	9.39/152.41	18.96/1199.83	3.56/53.73	16.23
A	20	100	7453	5.67/37.31	9.84/193.80	18.92/1737.64	3.33/46.57	19.70
A	20	200	18336	5.36/36.54	10.04/164.09	46.80/1210.21	8.74/33.12	16.34
A	20	300	13498	5.66/22.30	10.22/128.00	19.13/796.96	3.38/35.74	12.52
A	30	100	5529	5.24/21.68	9.77/142.40	18.46/1080.60	3.52/49.84	14.58
A	30	200	1865	5.27/22.49	9.99/117.00	18.53/776.48	3.52/34.53	11.71
A	30	300	7712	5.49/22.50	10.19/131.80	18.87/842.41	3.44/37.44	12.93
B	10	100	8196	5.63/37.53	10.56/201.94	20.18/1690.88	3.47/32.27	19.12
B	10	200	3486	5.58/37.26	10.17/208.03	19.98/1161.03	3.33/47.35	20.46
B	10	300	2206	5.58/37.05	10.07/188.30	20.63/1318.56	3.56/35.98	18.70
B	20	100	19700	5.63/36.85	10.70/177.87	20.30/1431.34	3.33/35.98	16.62
B	20	200	13688	5.59/36.89	10.30/179.90	20.04/1348.38	8.74/30.00	17.46
B	20	300	9090	5.62/36.45	10.48/160.40	20.23/1184.89	3.38/36.06	15.31
B	30	100	29161	5.62/22.39	10.64/145.73	20.29/1022.46	3.52/31.55	13.70
B	30	200	10895	5.65/22.47	10.78/129.38	20.69/938.10	3.52/30.38	12.00
B	30	300	18370	5.64/36.20	10.64/147.06	20.12/1001.68	3.44/21.39	13.82
C	10	100	8242	5.56/21.67	10.26/115.23	19.33/640.06	3.47/29.54	11.23
C	10	200	12504	5.97/22.23	9.94/143.04	19.89/871.48	3.33/39.20	14.39
C	10	300	10661	5.55/22.04	9.78/139.47	19.76/907.69	3.56/41.18	14.26
C	20	100	16243	5.77/21.38	10.01 /127.09	19.25 /621.89	3.33/29.09	12.70
C	20	200	11000	5.56 /22.43	10.44 /138.37	48.63 /746.52	8.74/33.28	13.25
C	20	300	1394	5.52 /20.04	9.97 /91.45	18.66 /812.21	3.38/40.53	9.17
C	30	100	21168	5.43 /21.34	10.13 /115.94	19.14 /628.95	3.52/29.47	11.46
C	30	200	21037	5.28 /21.68	10.02 /127.66	18.59 /780.23	3.52/35.99	12.74
C	30	300	29845	5.39 /11.71	10.00 /115.03	18.52 /763.45	3.44/65.20	11.50
D	10	100	4815	5.59 /36.79	10.31 /184.38	19.42 /1187.16	3.55/91.16	17.88
D	10	100	8331	6.00 / 36.70	10.00 /183.29	20.00 /1737.64	3.43/37.41	18.33
D	10	300	9177	5.90/36.24	10.40/162.07	21.00/1303.94	1.36/33.50	15.58
D	20	300	9201	6.00/36.24	10.40/170.00	20.00/1303.94	1.37/46.55	16.35
D	20	200	18512	5.62/36.45	10.55/165.76	49.15/1093.47	1.42/41.21	15.71
D	20	300	7392	5.56/22.52	10.04/149.30	18.80/811.99	1.36/35.72	14.87
D	30	100	20353	5.61/36.50	10.46/165.19	19.76/1151.62	1.77/43.45	15.79
D	30	200	21633	5.64/36.79	10.69/170.50	19.83/1117.80	3.39/41.57	15.95
D	30	300	7615	5.62/36.14	10.43/147.12	19.31/773.15	3.40/37.38	14.11

by extrusion without the need to further processes. In other words, energy consumption can be attained by selecting suitable configuration of the twin screw extruder.

Fiber Geometry

The results of processing effect on the fiber geometry are classified to two parts. The first part discusses the results of the extruder configuration on the final composite. The second part presents the change in the measured fiber geometry from one element to another.

Effect of Extruder Configuration on the Final Fiber Length/Diameter. Table III lists the measured fiber length and diameter using the QICPIC/M8 and M6 modes mentioned in "Samples for Fibre Geometry Development Along Extruder Length". Table III shows the median value (×50%) from the accumulated frequencies curve as well as the ×10 and 90% for both the fiber diameter and fiber length. Figure 9 shows an example for the cumulative distribution curves collected for fiber length using PP/10% flax at 100 rpm regarding all the studied extruders.

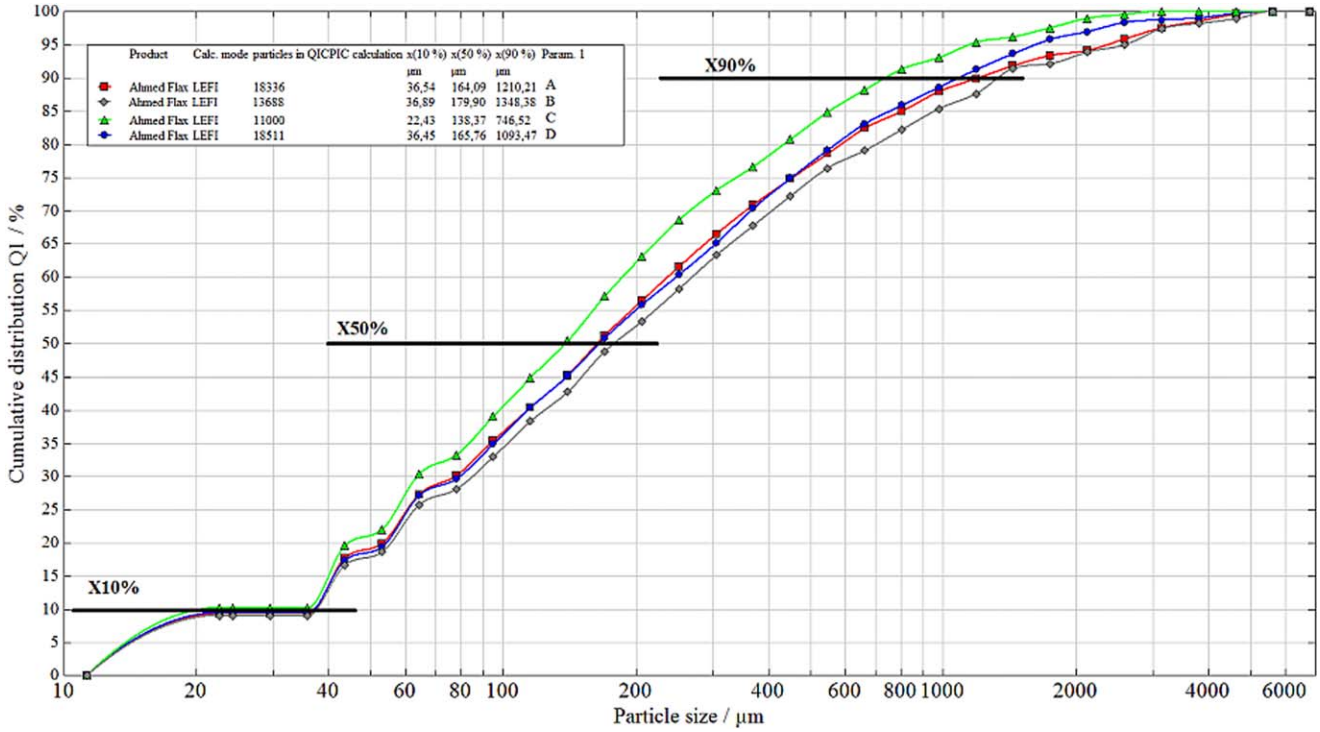

Figure 9. PP/20% flax at 200 rpm accumulative distribution curves of fiber length using Qicpic M8 mode for extruders A-B-C-D. [Color figure can be viewed in the online issue, which is available at wileyonlinelibrary.com.]

The *x* axis of the curve is logarithmic scale while the *y* axis shows the accumulation distribution curve in 'Q1' mode. 'Q1' mode is the first moment of the statistical distribution.[17] The value of ×90/×10 shows the convergence of the fiber dimension around the median curve. It will be called later the "homogeneity factor". The more this factor is, the less the number of very short fibers which do not share significantly in load transfer. Besides, lower homogeneity factor leads theoretically to a wide band of failure process. This leads practically to an early start of the failure and hence more likely to a quick sample failure. Finally, the aspect ratio 'AR' is calculated by dividing the median fiber length to the median fiber diameter. As seen in Table III, the homogeneity factor ×90/×10 for fibers' diameters is very small in comparison with that of fiber lengths. This suggests that the fiber diameter does not change drastically by the different processing parameters; namely, the fiber content and the extruder speed. On the other side, the fiber length is intensively affected with the above-mentioned processing parameters. Therefore the aspect ratio calculated will definitely have the same trend of fiber length. This slight change in fiber diameter implies also that the fibrillation is not so much affected by the selected extruder configuration because the fibers are quickly

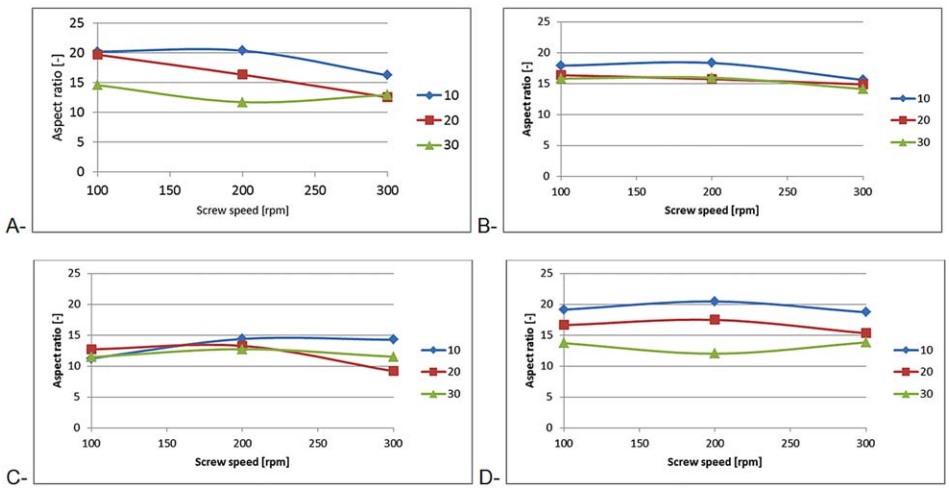

Figure 10. Aspect ratio of the extracted fibers using Qicpic M8 and M6 modes for length and diameter, respectively, regarding all extruders configurations A-B-C-D. [Color figure can be viewed in the online issue, which is available at wileyonlinelibrary.com.]

a- b-

Figure 11. A sketch shows the fiber in (a) tangled case with high aspect ratio and (b) relatively oriented fibers with low aspect ratio.

fibrilled or due to the dominace of the elementary fine small fibers on the statistical analysis. Irrespective of the reason is the fiber diameter is reduced slightly along the extruder. Hence, the quality of mixing and incorporating the fibers into the host polymer matrix plays the greater role in strength changing. So the claim of improving the mechanical properties by higher aspect ratio should be reconsidered. As increasing the aspect ratio implies the decrease of diameter and/or increase of length. From the above-mentioned results, the fiber diameter is not significantly affected by the design of the extruder configuration. So the remaining function in designing an extruder layout is to keep fiber length as long as possible. Taking into consideration that this point also assumes the fiber straightness which will be discussed later.

Figure 10 shows the aspect ratio calculated for the extruded materials at all configurations, fiber contents and all speeds. As seen in Figure 10, aspect ratios of 10% are always bigger than those of 20 and 30%. Thus, indicates the effect of the rubbing between the interacting fibers during extruder and their mutual damaging on their lengths. This is explained briefly in Nilsson,[18] where the fiber surface length is characterized with the presence of the dislocations like kink bands. These kinks represent weak points in fibers which are prone to break up to shorter ones. The effect of speed appears significant at all fiber contents in extruder configuration (A), where negative trend is obvious. For the 10% in case of (A), the aspect ratio decreases from almost 20 to 16, while the more fiber content of 20% shows more reduction where it drops from 19.7 at 100 rpm to 12.5 at 300 rpm. At 30% fiber content in case of (A), the aspect ratio suffers more reduction in fiber length even at 100 rpm where it is only 14.5 and then continues dropping to 12.5 at 300 rpm.

This behavior is repeated but to a lower extent in case of configuration (B). This is expected because of the lower kneading elements which exist in this configuration. In configurations (C) and (D), the trend of aspect ratios is almost stable and independent from the fiber content. However, the aspect ratios lie in the range of [10–15] values which is almost 25% less than that of extruder (A) and (B). Screw (D) shows again the dependence of fiber aspect ratio on the fiber content where higher fiber content leads to a reduction in fiber aspect ratio. The 10% has a high aspect ratio which is comparable to that of configuration (A). The speed does not play a significant role with configuration (D).

What is important in Figure 10 is the fact that configuration (C) has the least aspect ratio values which is not expected due to the composite high mechanical properties. This result is also in agreement with Beagrand.[14] The fiber aspect ratio is not the only key factor which defines the corresponding mechanical properties. Even lowest aspect ratio shows better strength. This can be understood by recalling the fact that the flax fiber of low flexural stiffness and high aspect ratio does not work as expected in a unidirectional load-bearing behavior, see Figure 11. The tangled form of the flax fiber reduces the benefit of high aspect ratio. On the other way, short fibers may act better since the efficiency of load bearing in an oriented direction will be definitely increased. The microscopic study afterwards will investigate this claim.

It is interesting to see the effect of using 'Q2' modus by analysis. 'Q2' is the second moment of the statistical analysis where the fiber of larger area (length × diameter) has more weight than fiber of less area. Figure 12 shows the difference between 'Q1' and 'Q2' analysis modus. As obvious, 'Q2' modus shows aspect ratio about 2–5 times more than that of 'Q1' modus. The trend lines in case of 'Q2' modus is more divergent as shown by 'Q1' modus. The ranking (high to low) of aspect ratio using 'Q2' has the order of A-B-D-C. This means implicitly that the 'A', 'B', and 'D' extruder configurations have a wide range of fiber dimensions whereas the configuration 'C' has more convergent fiber dimensions. Hence, 'C' has the least increase in aspect ratio from 'Q1' to 'Q2' a lower share of trivial fibers. This note represents an advantage for the 'C' configuration with its MPE elements.

Development of Fiber Length/Diameter Along the Different Extruder Configurations. ***Dynamic image analysis.*** As mentioned in "Samples for Fibre Geometry Development Along Extruder Length", the extruder is stopped during running at

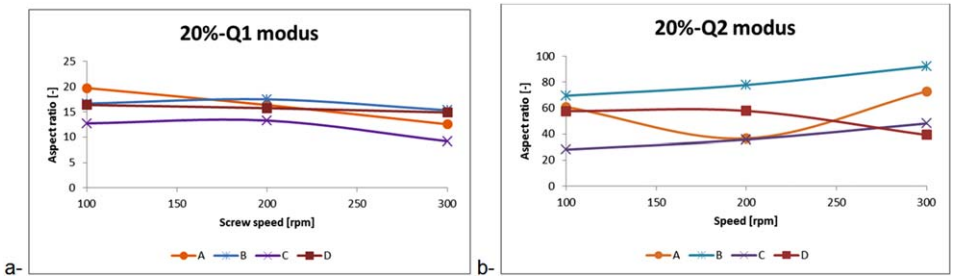

a- b-

Figure 12. Effect of the statistical analysis modus on the aspect ratio of 20% flax fiber content. (a) Q1, (b) Q2. [Color figure can be viewed in the online issue, which is available at wileyonlinelibrary.com.]

Table IV. Qicpic Measurements and Statistical Analysis of Fiber Dimensions at 30% Wf and 200 rpm for the All Studied Extruders (A, B, C, D)

Extruder	Position (mm)	Number of fibers	Diameter/ Length (μm) ×(10%)	Diameter/ length (μm) ×(50%)	Diameter/ length (μm) ×(90%)	×90/×10 Regarding length	AR
A	113.33	543	5.61/40.02	10.69/218.40	26.11/1579.88	39.48	20.43
A	140.00	5452	5.60/38.18	11.38/217.67	25.01/2475.40	64.83	19.12
A	200.00	7071	5.52/36.73	9.73/197.14	49.80/1857.82	50.58	20.26
A	246.67	7351	5.50/37.12	9.58/225.96	48.48/2607.05	70.23	23.59
A	280.00	5697	5.58/39.66	10.18/340.56	51.97/3729.22	94.03	33.45
A	306.67	11537	5.54/38.42	9.84/263.74	19.83/2141.19	55.73	26.80
A	440.00	6394	5.60/36.67	10.31/167.94	22.60/1425.76	38.88	16.29
A	460.00	9645	5.55/36.74	9.92/181.38	19.92/1376.46	37.46	18.28
A	473.33	6998	5.62/36.95	10.59/179.04	23.96/1373.29	37.17	16.91
A	646.00	1865	5.27/22.49	9.99/117.00	18.53/776.48	34.53	11.71
B	126.67	7510	5.49/42.78	9.52/201.94	20.34/4554.01	106.45	21.21
B	146.67	8042	5.56/37.13	10.09/231.51	20.67/2599.25	70.00	22.94
B	266.67	14181	5.55/37.09	9.89/210.25	19.55/1695.09	45.70	21.25
B	293.30	11616	5.62/38.25	10.40/237.90	20.44/3415.88	89.30	22.88
B	400.00	14553	5.55/36.37	9.90/167.92	19.34/1346.24	37.02	16.96
B	426.67	25557	5.59/36.44	10.26/164.77	19.71/1229.71	33.75	16.06
B	646.00	10895	5.65/22.47	10.78/129.38	20.69/938.10	30.38	12.00
C	113.33	7481	5.68/40.31	19.43/443.11	20.35/2445.74	60.67	22.78
C	126.67	3691	5.49/38.02	20.62/422.12	20.30/2330.09	61.29	20.47
C	153.33	1455	5.50/37.25	15.75/363.73	20.21/2007.82	53.90	23.09
C	166.67	2311	5.47/36.35	13.26/304.96	20.08/1928.32	53.05	22.99
C	193.67	981	5.39/36.11	12.18/249.98	20.03/1838.21	50.91	20.52
C	206.67	765	5.40/35.01	12.16/233.83	20.08/1754.82	50.12	19.23
C	233.33	1487	5.40/33.19	10.70/223.53	20.00/1683.38	50.72	20.89
C	246.70	3647	5.51/34.10	12.47/219.61	19.97/1379.93	40.47	17.62
C	393.30	2557	5.39/35.08	14.82/211.48	20.10/1290.72	36.79	14.27
C	420.00	608	5.31/33.89	12.93/203.87	19.95/1233.91	36.41	15.77
C	433.30	1287	5.29/33.24	12.29/203.74	19.90/1212.24	36.47	16.58
C	453.30	1378	5.28/35.14	10.76/200.40	19.88/1167.36	33.22	18.63
C	646.00	21633	5.64/36.79	10.69/170.50	19.83/1117.80	41.57	15.95
D	113.33	5899	5.50/39.04	9.65/371.09	19.55/3558.90	91.16	38.45
D	166.67	4055	5.50/36.19	9.63/170.68	18.86/1353.81	37.41	17.72
D	206.67	600	13.83/20.69	9.65/108.68	18.78/693.13	33.50	11.26
D	246.67	7945	13.77/22.08	9.66/157.47	18.87/1027.90	46.55	16.30
D	380.00	18632	13.98/22.00	10.32/127.39	19.90/906.71	41.21	12.34
D	413.30	4980	13.86/35.90	9.91/149.16	18.83/1282.17	35.71	15.05
D	433.30	10482	10.35/21.63	9.60/132.96	18.27/939.77	43.45	13.85
D	446.67	10486	5.56/22.42	9.99/149.21	18.82/932.08	41.57	14.94
D	446.67	7460	5.48/21.12	9.45/136.64	18.63/789.39	37.38	14.46
D	646.00	21037	5.28/21.68	10.02/127.66	18.59/780.23	35.99	12.74

30% fiber content and 200 rpm conditions. The extruder is drawn from the machine body and samples are taken after each element. Samples are dissolved. Fibers are extracted and measured using Qicpic. Table IV lists the diameter and length of the fibers at three cumulative levels; namely, 10, 50, and 90%. Fiber diameter decreases slightly from one element to another. This is interpreted earlier by the insignificant effect of the extruder configuration on the fiber diameter either due to the quick fibrillation or due to the huge amount of elementary fibers which are considered in the statistical calculation. Therefore focus will be asserted on the fiber length and its development. The convergence of the fiber distribution is represented by the

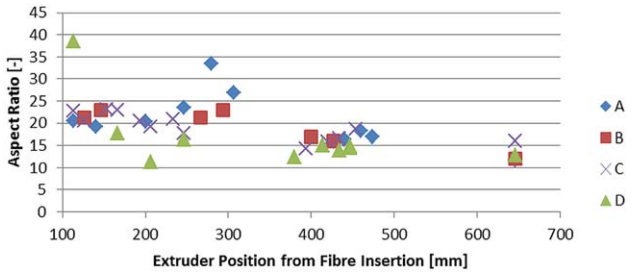

Figure 13. Fiber aspect ratio along the different extruders at 30% Wf and 200 rpm. [Color figure can be viewed in the online issue, which is available at wileyonlinelibrary.com.]

quotient (×90/×10) where the fiber convergence is becoming better when this quotient is getting decreased. Table IV presents the results of this quotient as well as the aspect ratio.

Table IV shows numerically the effect of the element type. In extruder 'A', the fiber length at 50% accumulative density function decreases gradually. A fluctuation in fiber length takes place at the end of the kneading phase (positions E and F) where the length increased. This may be attributed to the fibrillation and longitudinal decohesion of fibers. But this should be accompanied by a reduction in diameter which is not the case. So this can be better understood by recalling the fact that short fibers measuring depend on the quality of their dispersion in the pressurized air. In other words, fibers after kneading are severely shortened and damaged so that they are not captured by the measuring system to be measured. After that, drop in fiber length is obvious along the transport element due to temperature and shearing (see the difference in readings of ×50 between the last two positions 473.3 and 646.0 mm). In extruder 'B', the reduction, no fluctuation or big drop is observed after the kneading phase. This may be attributed to the few kneading elements in comparison with the doubled number of kneading elements in extruder 'A'. A drop in fiber length is observed again along the transport elements (see the difference between positions D and E, 293.3 and 400 mm, respectively. In extruder 'C', a smooth reduction in fiber length is observed. While in extruder 'D', a drop is observed in the fiber length after the first and the second teeth block elements. After that, stability in behavior is observed.

Figure 13 shows the development of the aspect ratio for all extruders. It is clear that aspect ratio reduces along the extruder

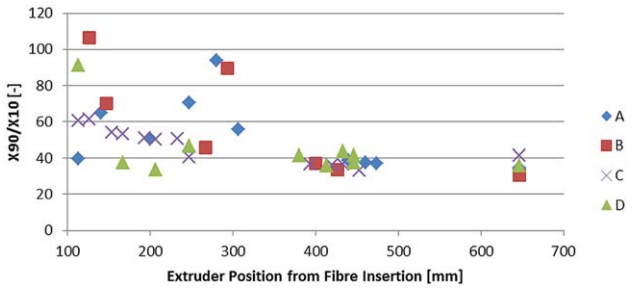

Figure 14. ×90/×10 quotient (regarding fiber length) along the different extruders at 30% Wf and 200 rpm. [Color figure can be viewed in the online issue, which is available at wileyonlinelibrary.com.]

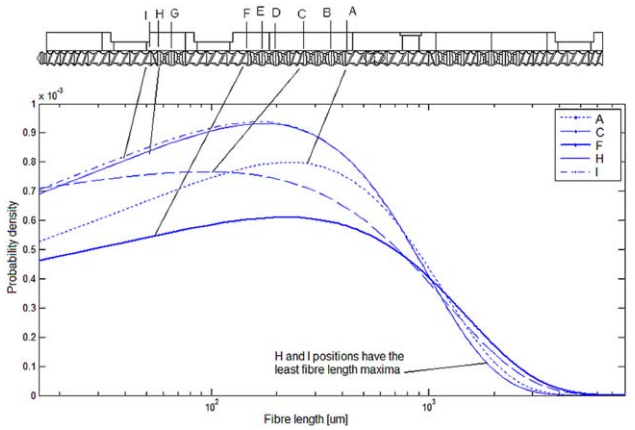

Figure 15. Weibull distribution of the fiber length along the extruder 'A' at 30% Wf and 200 rpm. [Color figure can be viewed in the online issue, which is available at wileyonlinelibrary.com.]

in general, but extruder 'C' preserves a stable behavior of AR. Also extruder 'A' where more kneading elements exist, shows high AR at the beginning as a better fibrillation is reached (see that ×90/×10 is more homogeneous and small for 'A' in comparison with 'B'). Also it is worth to note that the aspect ratio of extruder 'D' is always less than those of the others especially at the beginning. This presents the effect of the teeth elements where fibers are cut mechanically and not only due to decohesion of fibers under temperature and shearing.

Figure 14 shows ×90/×10, regarding fiber length only, to check the homogeneity of the fiber length distribution along the extruder length. The quotient is reduced to one third indicating homogeneity in the distribution and more convergence. From both Figures 13 and 14, it is obvious that stability of AR and ×90/×10 is reached in case of extruders 'C' and 'D' after short extrusion length without much need to the kneading elements phase. This suggests the possibility of using extruders with lower L/D ratio.

Figure 15 shows an example of the fiber length measurements along the extruder 'C' at different positions corresponding to the mounted elements. As obvious, the cumulative probability function, which is marked by 'A', is totally diverse for the fibers just entering the extruder. After passing by first kneading element, the cumulative distribution is retreated indicating smaller fiber length and more convergence. This behavior is increased by passing to the following kneading elements. Kneading at the end increases the convergence obviously. The data from the all elements at all extruders are collected and a Weibull distribution is selected[12] to describe the behavior of fiber length. The probability density function of Weibull distribution is given in eq. (5) where 'a' and 'b' are the scale and shape factors, respectively.

$$f(x)=b\frac{x^{b-1}}{a^b}e^{-\left(\frac{x}{a}\right)^b} \quad (5)$$

Using fitting tools of MATLAB, the Weibull parameters are calculated for the measured fiber length distributions. Table V lists the 'a' and 'b' parameters. These parameters are used again to plot the hypothetical Weibull density functions along the extruder length as shown in Figures 15–18. These distributions

Table V. Weibull Parameters of the Fiber Length Distribution Along Extruders (A, B, C, D) at 30% Wf and 200 rpm

Extruder	Position (mm)	*a*	*b*	Extruder	Position (mm)	*A*	*b*
A	113.33	931.40	1.22	B	126.67	2403.90	0.79
A	140	1416.30	1.00	B	146.67	1490.10	1.00
A	200	1078.80	1.08	B	266.67	994.80	1.16
A	246.67	1490.60	0.99	B	293.3	1910.70	0.92
A	280	2145.00	1.01	B	400	787.80	1.16
A	306.67	1258.10	1.16	B	426.67	721.80	1.20
A	440	831.50	1.13	B	646	553.40	1.22
A	460	808.70	1.19				
A	473.33	806.10	1.18				
A	646	458.70	1.28				
C	113.33	1452.60	1.42	D	113.33	2069.40	1.07
C	126.67	1383.80	1.42	D	166.67	793.00	1.16
C	153.33	1192.70	1.42	D	206.67	409.90	1.31
C	166.67	1144.60	1.31	D	246.67	609.40	1.29
C	193.67	1085.40	1.21	D	380	535.30	1.23
C	206.67	1035.00	1.20	D	413.3	745.60	1.12
C	233.33	992.80	1.20	D	433.3	555.30	1.24
C	246.7	818.10	1.32	D	446.67	552.80	1.33
C	393.3	765.10	1.34	D	446.67	468.30	1.39
C	420	731.40	1.35	D	646	462.40	1.34
C	433.3	718.80	1.36				
C	453.3	691.70	1.38				
C	646	659.20	1.28				

can help in modeling the fiber length and the effect of the extruding elements. Figure 15 shows the Weibull curves of extruder 'A' where a fluctuation is observed in the positions (A, C, F). The curve median peak fluctuates by increasing the kneading indicating different modes of fibrillation and fiber breaking. Then, a stability takes place where low left biased medians appear at positions (H, I). The reverse element does not make a significant effect on fiber length as expected.

The behavior is interesting in extruder 'B' shown in Figure 16. The curve medians change slightly at the first and second kneading phases (only two elements at a time). Then after a relatively long transport by the transport elements and passing another kneading pass, the curve medians are shifted towards left again.

The most smooth transitional behavior is shown in extruder 'C' using MPE elements where the curve medians are shifted

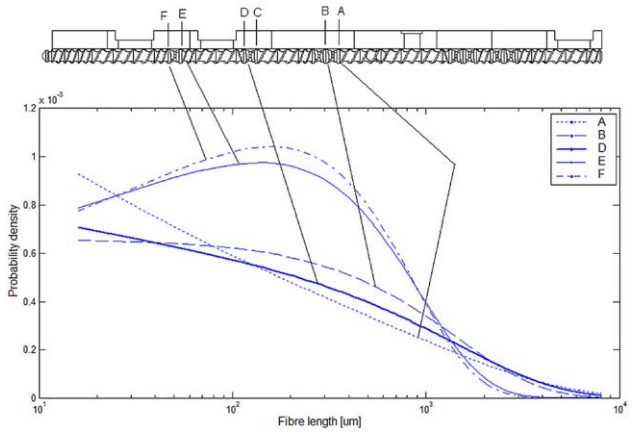

Figure 16. Weibull distribution of the fiber length along the extruder 'B' at 30% Wf and 200 rpm. [Color figure can be viewed in the online issue, which is available at wileyonlinelibrary.com.]

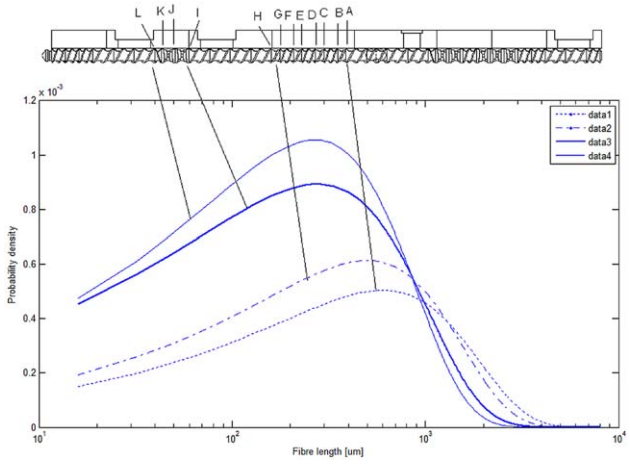

Figure 17. Weibull distribution of the fiber length along the extruder 'C' at 30% Wf and 200 rpm. [Color figure can be viewed in the online issue, which is available at wileyonlinelibrary.com.]

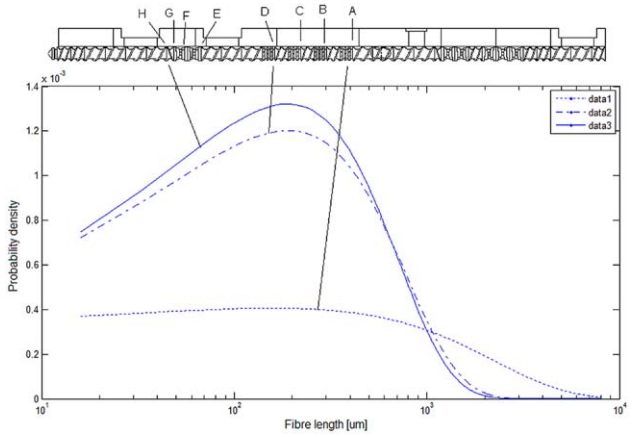

Figure 18. Weibull distribution of the fiber length along the extruder 'D' at 30% Wf and 200 rpm. [Color figure can be viewed in the online issue, which is available at wileyonlinelibrary.com.]

gradually to the left firstly by the MPE element and then more remarkably by kneading elements. The behavior is slightly different in extruder 'D' shown in Figure 18, where the mechanically cut fibers show a flat plateau at the beginning and then great convergence after kneading. This can be thoroughly seen in Table IV where the quotient ×90/×10 values reduced drastically from 91 before the first element to almost 30 starting from the second element.

Microscopic. The possible effect of the large number of fine fibers on the statistical calculation leads to the following questions. Can we disregard the fine small fibers and study the effect of the larger size fibers. This can be done by selecting a minimum threshold fiber length/diameter to be considered. Another point questions the effect of the dissolving technique on the fiber shape and impregnation of the PP matrix around the fibers. Therefore, the microscopic examination is carried out on the samples using a normal optical microscope. The fiber lengths and diameters are also measured at different locations using the magnification shown in Figure 19 to have an overall look with

Figure 19. Microscopic sample of extruder (A) at 200 rpm and 30% Wf. [Color figure can be viewed in the online issue, which is available at wileyonlinelibrary.com.]

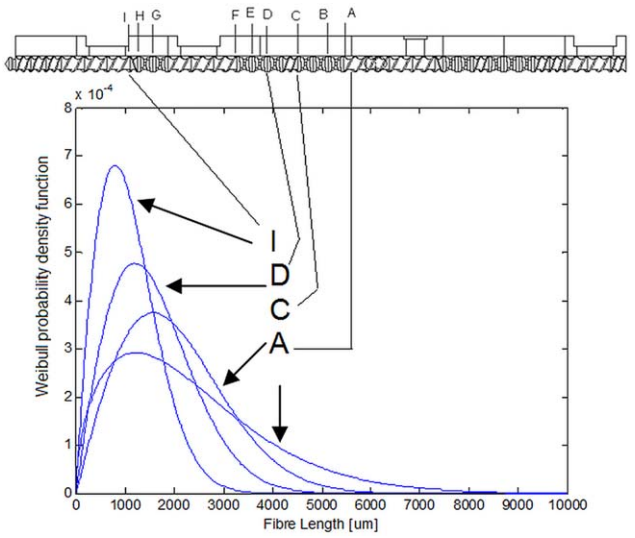

Figure 20. Development of fiber length distribution on extruder (A) at 200 rpm and 30 wt % flax. [Color figure can be viewed in the online issue, which is available at wileyonlinelibrary.com.]

large and small size fibers. As expected, most of the fine fibers are not captured because they are either too fine or are attached on the surface of the large size fibers. It is worth to note that the fiber diameter is expected to be larger than the actual fiber diameter due to the sample film pressing during preparation. It is also obvious that despite pressing, most of the fibers are not straight. This assures the assumption of the low flexural strength of the flax fiber which affects in turn its loading transfer efficiency. Readings of 100 fibers are taken and processed to find their Weibull distribution as shown in Figure 20 for the development of fiber length along the extruder (A). The medians-as expected- are shifted to higher values. For instance, the median values in Figure 15 are ranging from 170 to 350 μm and those in Figure 20 ranging from 800 to 1500 μm. The focus given to the bigger fibers is most likely the reason for this difference. This can be ensured by the more remarkable reduction of the median in a logic order at the positions (A, C, D, I) consequently.

Anyway, this topic of the difference in measuring techniques and interpretations requires a lot of work using other types of dispersive media like wet dispersion for instance to compare the results and then to decide the best code of practice of measuring fibers after extraction.

This work can also be developed to include the effect of the extruder configurations on the consumed specific mechanical energy at different speeds and different fiber contents. However, this is intended to be in a separate future study.

CONCLUSION

The effect of the extruder configuration and the processing parameters on the PP/flax composites can be concluded in the following aspects regarding:

- The mechanical properties;
- The dimensions of the extracted fibers after extrusion;

- The development of fiber dimensions and the homogeneity of the dimensions distribution along the extruder in addition to the statistics describing the fiber dimensions distribution.

Mechanical Properties

The ranking of extruder configurations from the lowest mechanical properties to the best is as follows: B-A-D-C. The strain at break is oppositely ranked. The improvement in E-modulus and tensile strength is attributed to either of the following reasons: Higher fiber aspect ratio, or due to more available sites on the fiber surface area to couple the polymer with the natural fiber. The fiber measurement supported the second reason.

Speed effect on E-modulus is insignificant but it has a significant negative effect on strength in the speed range [100–200] rpm. On the other hand, the significance of speed–strength relation is getting weaker at 30% wf. This is explained in terms of the rubbing between the interacting fibers. Speed effect is believed to suffer from two contradicting factors namely improving the fibers' distribution by increasing the speed and damaging the fibers on the other side.

Increasing the fiber content improves the mechanical strength, but in a nonlinear relation.

Comparing the mechanical properties of the injection molded samples with the extruded samples suggests that selecting an appropriate configuration like extruder 'C' and 'D' would save further processing needed to improve the polymer–fiber adhesion.

Extracted Fiber Measurement After Extrusion

Fiber diameter is reduced only almost 10% in average. On the other side, the fiber length is getting shorter. This results in AR reduction. This implies that the reason of improving the mechanical properties is not the enhancement of fiber aspect ratio, but mainly the better fiber distribution and the more available sites for coupling. This claim of disregarding the aspect ratio is not general but it may be valid for the flax fiber which is characterized with its low flexural stiffness.

In configurations 'A' and 'B': Increasing the speed and hence the shearing force resulted in significantly shorter fiber length and smaller aspect ratios especially at higher fiber contents. The median statistical value for the aspect ratio is reduced from almost 20 μm at 100 rpm to 16 and 12.5 μm for 10 and 30%, respectively at 300 rpm. This effect of speed is not significant in case of configurations with special elements 'C' and 'D'.

Development of Extracted Fibers Dimensions Along Extruder Length and Statistics of Fiber Homogeneity

The stability of AR and $\times 90/\times 10$ is reached in case of extruders 'C' and 'D' after short extrusion length without much need to the kneading elements phase. This suggests the possibility of using extruders with lower L/D ratio.

Definition of the Weibull distribution parameters is still debatable depending on the measurement technique. However, a smooth development in fiber length is mostly seen by configuration 'C' then 'D'. Log normal distribution can also be discussed in future.

As a summary, this work shows the effect of the extruder configurations on the attained properties. This work proves that the common concept of aspect ratio–strength relationship is not in all cases valid.

ACKNOWLEDGMENTS

Thanks are given to the Fachagentur Nachwachsende Rohstoffe e.V. (FNR) agency for financing. Also thanks are due to Prof. Gerhard Ziegmann for his help in facilitating the work in TU-Clausthal.

REFERENCES

1. Bogoeva-Gaceva, G.; Avella, M.; Malinconico, M.; Buzarovska, A.; Grozdanov, A.; Gentile, G.; Errico, M. *Polym. Compos.* **2007**, *28*, 98.
2. Van de Velde, K.; Kiekens, P. *J. Thermoplast. Compos. Mater.* **2001**, *14*, 244.
3. El-Sabbagh, A.; Steuernagel, L.; Ziegmann, G. *J. Biobased Mater. Bioenergy* **2012**, *6*, 346.
4. Saheb, D.; Jog, J. *Adv. Polym. Tech.* **1999**, *18*, 351.
5. Gibson, R. Principles of Composite Material Mechanics; McGraw-Hill: New York, ISBN 0–07-023451-5, **1994**.
6. Krenchel, H. In Fibre Reinforcement. Akademisk Forlag: Copenhagen, **1964**.
7. Kelly, A.; Tyson, W. *J. Mech. Phys. Solids* **1965**, *13*, 329.
8. Bos, H. Thesis, May 27, TU Eindhoven, **2004**.
9. El-Sabbagh, A.; Steuernagel, L.; Ziegmann, G. *Polym. Compos.* **2009**, *30*, 510.
10. Glasser, W.; Taib, R.; Jain, R.; Kander, R. *J. Appl. Polym. Sci.* **1999**, *73*, 1329.
11. Baiardo, M.; Zini, E.; Scandola, M. *Composit. Part A* **2004**, *35*, 703.
12. Andersons, J.; Sparnins, E.; Joffe, R. *Polym. Compos.* **2006**, *27*, 221.
13. El-Sabbagh, A. Effect of Twin Screw Extruder Layout on Natural fibre Polymer Composites, PEDD8, 9–11 March, Cairo **2010**.
14. Beaugrand, J.; Berzin, F. *J. Appl. Polym. Sci.* **2012**, *128*, 1227.
15. El-Sabbagh, A.; Steuernagel, L.; Ziegmann, G. *J. Appl. Polym. Sci.* **2009**, *111*, 2279.
16. Xue, L.; Tabil, L.G. *J. Polym. Environ.* **2007**, *15*, 25.
17. Roman, M.; Hinz, T. *LandbauforschungVoelkenrode* **2007**, *308*, 91.
18. Nilsson, T. Micromechanical Modelling of Natural Fibres for Composite Materials, Thesis, Lund University, Sweden, **2005**.